

## The influence of ball shot material on the surface properties of vibratory shot-peened parts

Agnieszka Skoczylas<sup>1\*</sup>, Kazimierz Zaleski<sup>1</sup>

<sup>1</sup> Department of Production Engineering, Mechanical Engineering Faculty, Lublin University of Technology, Nadbystrzycka Street 36, 20-618 Lublin, Poland

\* Corresponding author's e-mail: a.skoczylas@pollub.pl

### ABSTRACT

The samples of C45 steel and heat-treated samples 100Cr6 steel were subjected to a vibratory shot peening (VSP) process conducted with variable shot peening conditions. The variable parameters of the process were: ball material (100Cr6 and HS18-0-1) and vibratory shot peening time ( $t = 1$  min and  $t = 15$  min). Surface topography, surface roughness (3D parameters), surface microhardness, and residual stress were examined before and after the shot peening process. A multi-factor ANOVA analysis was performed for the surface roughness parameter  $R_a$ . For the C45 steel samples, the use of vibratory shot peening leads to increased surface roughness compared to that before shot peening. The 3D surface roughness parameters of 100Cr6 steel are lower after the vibratory shot peening process than before VSP. The effect of vibratory shot peening is increased microhardness, which is greater for the C45 grade of steel than for 100Cr6. After VSP, compressive residual stresses occur in the surface layer. The shot peening process conducted with the 100Cr6 shot produces surfaces with lower surface roughness than that obtained after shot peening with the HS18-0-1 shot, whatever the workpiece material and the time  $t$ . Regarding the physical properties of the surface layer (microhardness and residual stress), better results (a greater increase in the microhardness  $\Delta HV$  and a higher absolute value of the compressive residual stress  $\sigma$ ) were produced by the shot peening process conducted with HS18-0-1 balls.

**Keywords:** vibratory shot peening, ball material, surface roughness, microhardness, residual stress.

### INTRODUCTION

The quality of manufactured parts depends, among other things, on the properties of their surface layer. The condition of the surface layer formed during the manufacturing process affects the functional properties of products, such as material fatigue resistance, tribological wear and corrosion. Research by Liu showed that the changes in the surface layer of 2205 duplex stainless steel samples induced by ultrasonic rolling led to a several-fold increase in their high-cycle fatigue life [1]. The relationship between surface roughness and residual stresses and the fatigue strength of parts manufactured by various methods was investigated in [2]. The results of numerical and experimental studies on the effect of finishing parameters on fatigue wear were

reported in [3]. A study by Avcu et al. showed that the changes in the surface layer of titanium alloy induced by shot peening reduced the wear rate of the shot-peened surfaces [4]. Another study [5] found that the wear behaviour of agricultural machinery components depended on the welded layer material and operating conditions. The changes in the microstructure of the surface layer of AISI 316L stainless steel induced by conventional and severe shot peening increased the corrosion resistance of this steel grade [6]. Changes in the surface layer affecting the corrosion resistance of machinery components can be achieved by using appropriately selected laser radiation parameters acting on the surfaces of these components [7]. A study [8] demonstrated that residual stresses formed in the surface layer of alloy 600 specimens were an important factor influencing the stress

corrosion cracking of these specimens. A change in the surface layer resulting from a modification of finishing conditions can lead to a change in surface free energy (SFE), which is of great importance in bonding processes [9]. The results of SFE tests conducted on C45 steel specimens after slide burnishing in various liquids were presented in [10], while the authors of [11] investigated the influence of different processing methods for EN AW 2024 and EN AW 5083 aluminium alloys on the SFE of these materials.

To improve the performance of manufactured parts, mainly machinery components, strain hardening is often employed [12, 13]. If the deformation of the surface layer is a result of static impact of a smooth tool on the treated surface, this process is called burnishing [14, 15]. However, if the properties of the surface layer are changed as a result of the working tool's impact on the workpiece, this is referred to as shot peening [16, 17]. Good results in terms of surface layer properties and fatigue life can be achieved by using burnishing after prior shot peening [18].

As a result of shot peening, an increase in the microhardness of the surface layer and the formation of compressive residual stresses in the peened object are usually obtained [19, 20]. There may also be a change in the microstructure of the material being processed [21]. Depending on the type of material being shot peening and the technological conditions of the process, shot peening may result in an increase or decrease in surface roughness [22, 23]. Shot peening can also be used to remove burrs that form during machining and to round the edges of manufactured items [24]. The properties of the surface layer can be improved by dynamic interaction with the processing medium, in the form of metal or ceramic fibres, occurring during the brushing process [25, 26]. Brushing not only changes the condition of the surface layer, but can also remove existing surface defects [27].

The effects of shot peening depend not only on the parameters of the process, but also on the type of shot peening medium. In the streaming shot peening process, characterised by the impact of a stream of shot particles on the surface being treated, which are set in motion by mechanical or pneumatic devices, small balls or shots are used [23]. The authors of the study [28] used steel balls with a diameter of 1.2 mm in their research on the effect of shot peening in combination with low-temperature plasma nitriding and arc deposition

on wear resistance. Hotz et al. used ceramic beads with a diameter of 0.4 mm and 0.6 mm in their research on surface layer hardening of austenitic stainless steel samples in a shot peening process [29]. Various shot peening media, namely nutshell granules with dimensions of 0.45–0.8 mm, ceramic beads with a diameter of 0.125–0.25 mm, and stainless steel shot with a diameter of 0.4–0.9 mm, were used in studies of the effect of shot peening on the properties of the surface layer of Ti-6Al-4V [30]. An increase in the fatigue strength of AZ80 magnesium alloy samples was achieved by shot peening with glass beads with a diameter of 0.3 to 0.4 mm [31].

One type of shot peening is vibratory shot peening, which involves hitting loose peening elements on the surfaces of workpieces under the influence of vibrations in a closed working chamber in which these peening elements and workpieces are located [32, 33]. The workpieces are fixed “permanently” in the working chamber or placed on a rotating mandrel inside the working chamber [34]. During vibratory finishing, objects, especially small ones, can move freely in the vibrating working chamber, colliding with elements of the shot-peening medium [35, 36]. The elements of the medium used in the vibratory shot peening process are larger than those used in the jet shot peening process. In experimental studies conducted to train an intelligent vibratory shot peening system, 4 mm diameter balls made of AISI 420C stainless steel were used as the processing medium, which after special heat treatment had a hardness of HRC48÷52 [37]. Balls made of 100Cr6 bearing steel with diameters ranging from several to several millimetres are widely used in the vibratory shot peening process [33, 38]. Reducing surface roughness and improving the properties of the surface layer of vibratory shot-peened objects can be achieved by using a medium consisting of variously shaped elements made of materials such as silicon carbide, resin, corundum with dimensions ranging from 6 mm to 18 mm [35].

In previous studies on vibratory shot peening, much attention has been paid to the influence of the parameters of this process on the surface properties of the workpieces [35, 39]. The condition of the surface layer of objects after vibro-peening and shot peening was also compared [40]. It has been found that the properties of the surface layer of objects after vibratory shot peening depend on the degree of

filling of the working chamber with balls [38] and on the diameter of the bearing steel balls used as the processing medium [41]. However, there are no studies that would present the impact of the type of ball material, at a constant volume, on the variables under investigation. The aim of the research presented in this paper was to evaluate the influence of the specific weight of balls of the same diameter but made of different materials on the properties of the surface layer of vibration-shot peened samples.

## RESEARCH METHODOLOGY

The study used perpendicular samples with dimensions  $4 \times 15 \times 100$  mm made of two different engineering materials. It was C45 non-alloy steel and 100Cr6 bearing steel after heat treatment. Prior to vibratory shot peening, the samples underwent pre-treatment in the form of grinding. They were ground with a Norton Saint-Gobain aloxite grinding wheel type 8A60M7VS3 having the dimensions of  $400 \times 50$  mm. The following technological parameters were used: the cutting depth  $a_p = 0.05$  mm, cutting speed  $v_c = 20.00$  m/s, and emulsion as a cutting fluid. C45 steel is used for medium-duty machine components such as non-hardened gears, spindles, electric motor shafts and wheel hubs. Previous work [10] confirmed that this species is susceptible to burnishing and shot peening. 100Cr6 bearing steel is used in the construction of rolling bearings. It is often used to manufacture bearing components such as rings, balls, rollers or needles. It is also used for knives and tools. Table 1 presents the chemical composition based on the material data sheet and PN-EN ISO 683-17:2024-04, PN-EN ISO 683-1:2018-09 standards for C45 steel and 100Cr6 steel, which were ground before vibratory shot

peening. The samples made of C45 non-alloy steel were in a normalised state, while those made of 100Cr6 steel were heat treated. Heat treatment included hardening and two tempering processes. The microhardness for 100Cr6 steel was  $560 \pm 20$  HV0.5.

A mechanical-kinematic vibrator with a working chamber was used for the vibratory shot peening process. Cuboid samples with dimensions  $4 \times 15 \times 100$  mm were attached to the bottom of the working chamber. Next, the working chamber was filled with balls with a diameter of  $d_k = 12$  mm, the so-called “charge”. Two types of balls were used for vibratory shot peening. These were balls made of 100Cr6 bearing steel with a density of  $7.85 \text{ g/cm}^3$  and balls made of HS18-0-1 high-speed steel with a density of  $8.61 \text{ g/cm}^3$ . A constant vibration amplitude of  $a = 5$  mm, a vibration frequency of  $\nu = 2100$  1/min and two shot peening times of  $t_1 = 1$  min and  $t_2 = 15$  min were used. Figure 1 shows the station used for vibratory shot peening.

The stereometric properties of the surface layer were tested using a T8000RC 120–400 device manufactured by Hommel Etamic. The TKU300 tip, a device component equipped with a needle with a radius of  $r_k = 5 \text{ }\mu\text{m}$ , was used to measure the topography and roughness parameters of the surface. The surface area of  $4.0 \times 4.0$  mm was scanned. The 3D roughness parameters  $S_a$ ,  $S_z$ ,  $S_p$  and  $S_v$  were analysed and the  $R_a$  parameter was analysed using ANOVA. For each vibratory shot peening condition, 12 measurements of  $R_a$  surface roughness parameter were performed. Outliers (maximum and minimum) were rejected. The Vickers method was used to measure microhardness on the surface of the samples using a Leco LM 700at microhardness tester. The penetrator load was 500 g (HV0.5). The portable Theta-Theta EDGE diffractometer was used to

**Table 1.** Chemical composition of 100Cr6 and C45 steel according to the material data sheet and PN-EN ISO 683-17:2024-04 and PN-EN ISO 683-1:2018-09 standards

100Cr6										
Chemical composition (average), [%]										
C	Mn	Si	P	S	Cr	Mo	Cu	Al	O	Fe
0.9–1.05	0.15–0.35	0.25–0.45	max. 0.025	max. 0.015	1.35–1.60	max. 0.10	max. 0.30	max. 0.050	max. 0.0015	rest
C45										
Chemical composition (average), [%]										
C	Mn	Si	P	S	Cr	Ni	Mo	Fe		
0.48	0.74	0.36	0.011	0.01	0.09	0.02	0.002	rest		



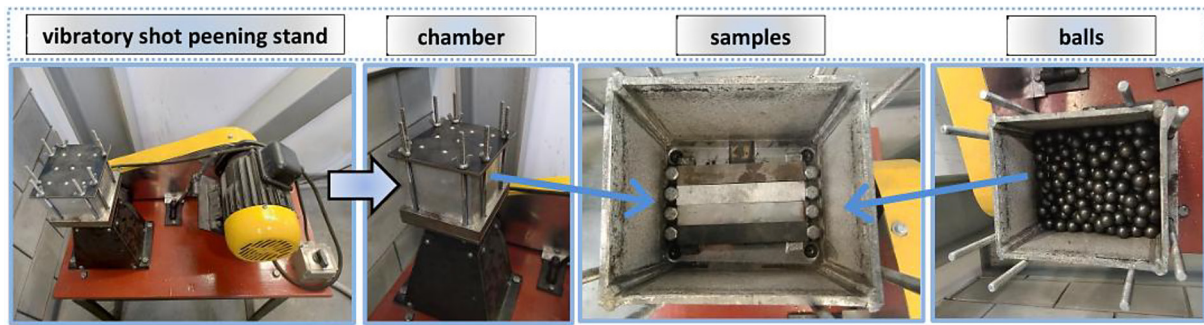


**Figure 1.** Test stand for vibratory shot peening

measure residual stresses. The measurement of residual stresses was performed in one direction. A chrome lamp as the X-ray source, a wand filter and a collimator with a diameter of 0.5 mm were used for the measurements. The X-ray exposure time was 30 seconds, the diffraction angle was  $11^\circ$ . The material model “unalloyed steel\_carbon steel” from the device library was used. The residual stress measurements were performed on the surface, so the penetration depth of the XRD beam is small. The measuring stations and devices used to measure the properties of the analyzed objects are shown in Figure 2.

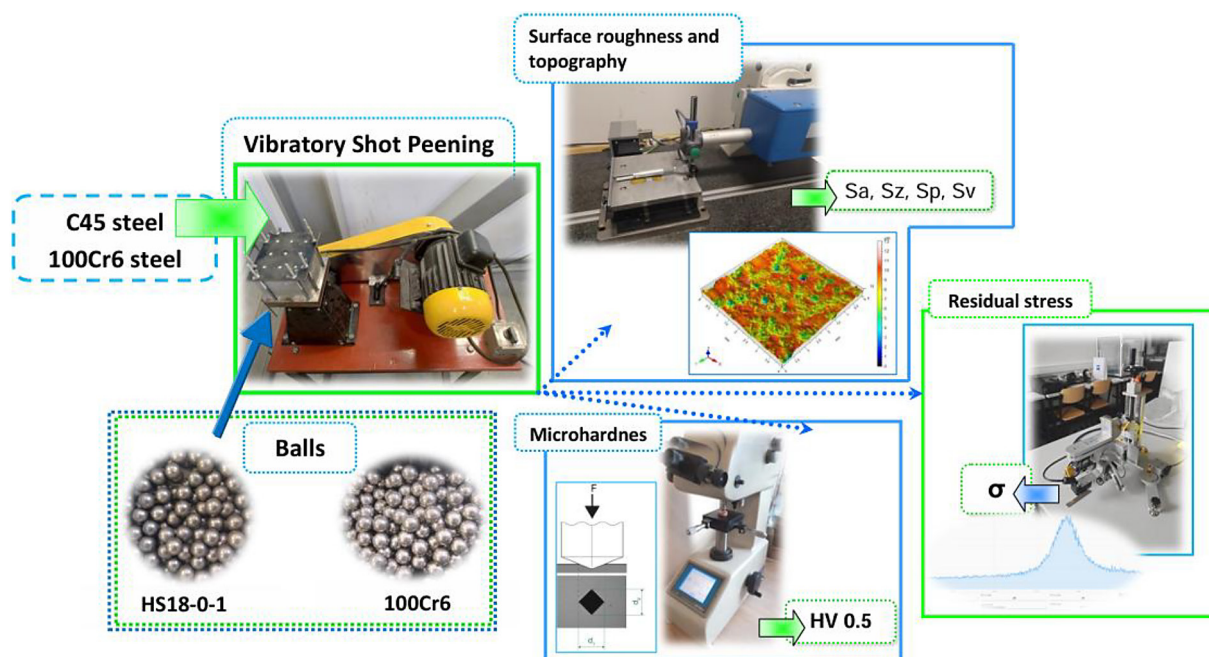
The study included a statistical analysis of the surface roughness parameter  $R_a$ . A two-factor ANOVA analysis was employed to demonstrate statistically significant differences and

interactions between dependent variables. Prior to the ANOVA analysis, the normality of the dependent variable distribution was tested by the Shapiro-Wilk test. The significance level was set equal to  $\alpha=0.05$ . The analyses were performed using Statistica version 13.

## RESULTS AND DISCUSSION

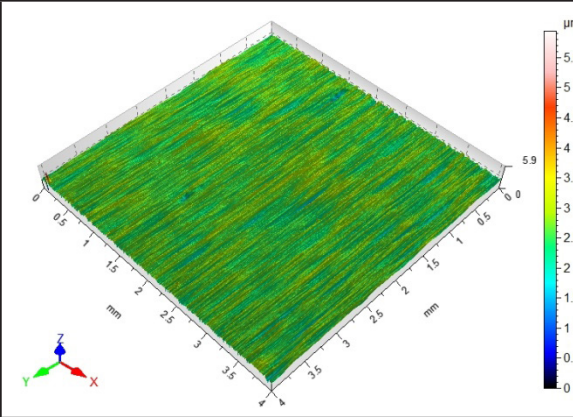
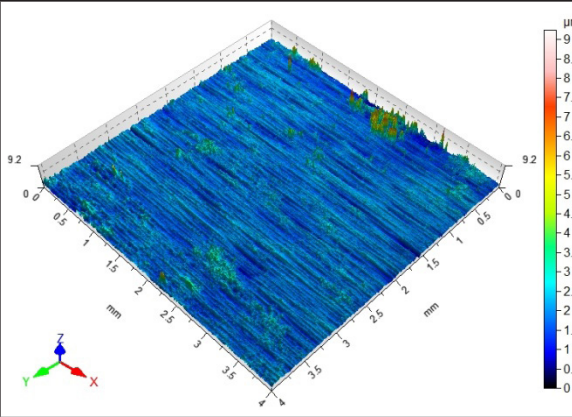
### Surface topography

Table 2 presents the surface topography of C45 and 100Cr6 steel samples before the vibratory shot peening process. For both tested materials, a unidirectional arrangement of micro-irregularities can be seen before shot peening. The micro-irregularities after the pre-treatment have a parallel



**Figure 2.** Testing stations used to measure the surface properties of C45 and 100Cr6 steel objects after vibratory shot peening with balls made of various materials

**Table 2.** Topography of the surface before VSP

C45	100Cr6
 <p> <math>S_a = 0.198 \mu\text{m}</math>; <math>S_z = 5.94 \mu\text{m}</math>  <math>S_v = 2.54 \mu\text{m}</math>; <math>S_p = 3.40 \mu\text{m}</math>; </p>	 <p> <math>S_a = 0.258 \mu\text{m}</math>; <math>S_z = 9.24 \mu\text{m}</math>  <math>S_v = 1.97 \mu\text{m}</math>; <math>S_p = 7.27 \mu\text{m}</math>; </p>

arrangement. The  $S_a$  parameter value for both materials is similar. Differences occur in the values of the  $S_z$ ,  $S_v$  and  $S_p$  parameters. For the 100Cr6 steel sample, sharp peaks can be observed on the surface (the  $S_p$  parameter is more than twice as high as for the C45 steel sample). For the C45 steel sample, the proportion of peaks and valleys in the maximum surface height is similar, which is not the case with the 100Cr6 steel sample, where the peaks dominate. The differences in the  $S_p$  and  $S_v$  parameters indicate that the heat-treated 100Cr6 steel is a difficult-to-machine material.

Vibratory shot peening resulted in a change in the surface topography (Tables 3 and 4). Regardless of the ball material, traces in the form of depression appear on the surface of C45 steel samples as a result of the balls hitting the sample (Table 3). Surface maps, regardless of the shot peening conditions, have a similar micro-irregularity pattern. Numerous peaks and valleys are visible, resulting from plastic deformation of the material due to impacts. In the case of 100Cr6 steel samples, micro-irregularities are cut off after pre-treatment, and despite vibratory shot peening, their unidirectional arrangement is still visible. For both engineering materials (C45 and 100Cr6 steel), surfaces shot peened with HS18-0-1 steel shot show a higher degree of deformation than those shot peened with 100Cr6 shot.

The micro-roughness pattern obtained for the C45 steel samples after vibratory shot peening with both 100Cr6 and HS18-0-1 balls is similar to the surface topography obtained in our previous work [38] and in a study [39]. Regarding the surface topography of vibratory shot-peened 100Cr6

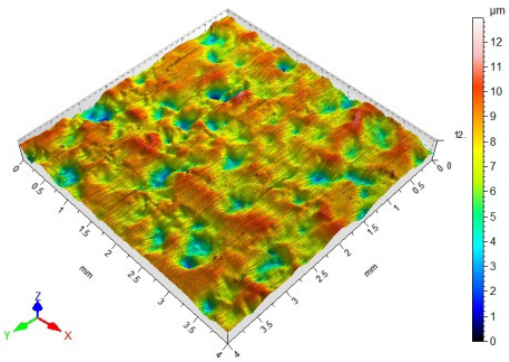
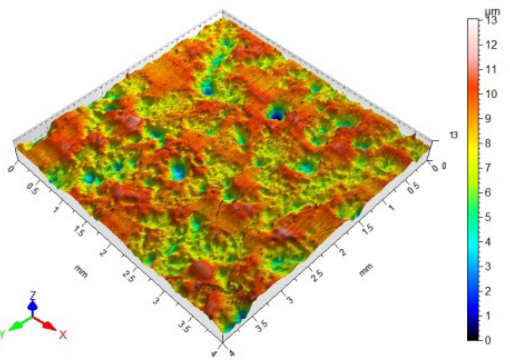
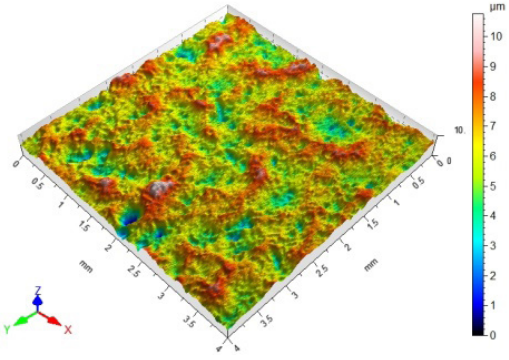
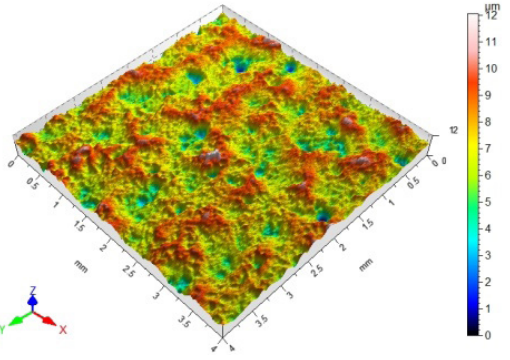
steel samples, similarities can be observed related to the results presented in [41], with micro-irregularities still visible after the pre-treatment.

### Surface roughness

For surface topography maps, 3D surface roughness parameters were generated and are presented in the graphs below as a function of the vibratory shot peening conditions used. Table 5 shows summary results of 3D surface roughness parameters. Figure 3 shows the  $S_a$  roughness parameter as a function of the vibratory shot peening parameters applied. In the case of C45 steel samples (Figure 3a), after vibratory shot peening, the  $S_a$  parameter increases, while for 100Cr6 samples (Figure 3b), it is lower than before shot peening. Similar changes were obtained for the  $S_z$  parameter (Figure 4). When analyzing the influence of the ball material on the  $S_a$  roughness parameter, it should be noted that for C45 steel samples, regardless of the vibratory shot peening time, and for 100Cr6 samples shot peened at  $t=15$  min, after VSP with HS18-0-1 balls, the  $S_a$  parameter has higher values. The difference ranges from 6% to 9%. In the case of 100Cr6 steel samples, for a shot peening time of  $t=1$  min, a lower  $S_a$  value was obtained after shot peening with HS18-0-1 balls than with 100Cr6 balls. It should be explained that the use of balls with a higher specific weight (balls made of HS18-0-1) at  $t=1$  min causes a “smoothing” effect on hard micro-irregularities, which are cut off rather than deformed. In the case of the roughness parameter  $S_z$ , the lowest value within the scope of the experiment was obtained



**Table 3.** Surface topography of C45 steel after VSP

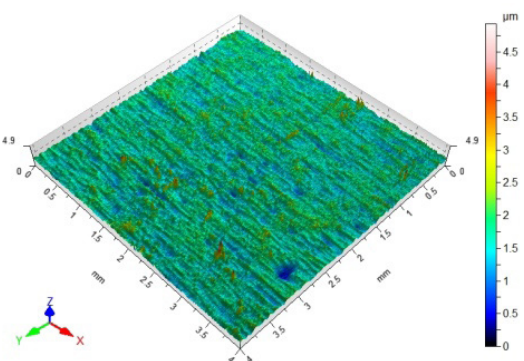
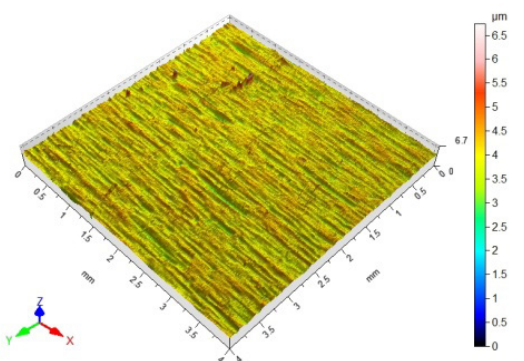
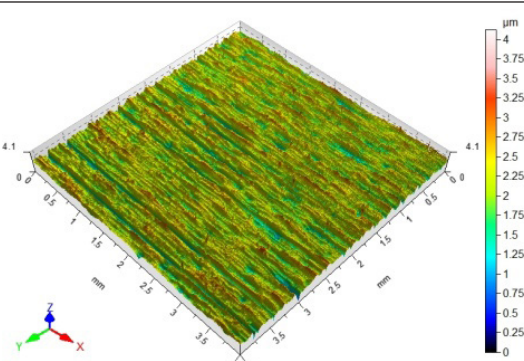
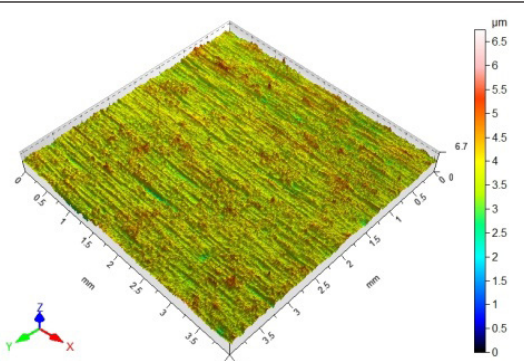
Time VSP t	Ball material: 100Cr6	Ball material: HS18-0-1
1	 <p>Sa = 1.08 μm; Sz = 13 μm; Sv = 7.79 μm; Sp = 5.16 μm;</p>	 <p>Sa = 1.08 μm; Sz = 13.1 μm; Sv = 8.45 μm; Sp = 4.53 μm;</p>
15	 <p>Sa = 0.943 μm; Sz = 10.80 μm; Sv = 6.36 μm; Sp = 4.40 μm;</p>	 <p>Sa = 1.01 μm; Sz = 12 μm; Sv = 7.39 μm; Sp = 4.66 μm;</p>

for samples made of 100Cr6 steel shot peened for  $t=15$  min with 100Cr6 balls. The Sz parameter for these conditions is 2.1 times lower than after the pre-treatment. An interesting result is obtained for a sample of 100Cr6 shot peened with HS18-0-1 balls for  $t=1$  min and  $t=15$  min, with a similar value of the Sz parameter. In the case of differences in the Sa and Sz parameter values depending on the ball material, greater differences were obtained for samples made of 100Cr6 steel than for C45. An increase in shot peening time from  $t=1$  min to  $t=15$  min causes an decrease in the Sa and Sz parameters for samples made of C45 steel and Sz for samples made of 100Cr6. It should be explained that as the shot peening time increases, the balls strike the same place repeatedly, causing multiple deformation of the same areas. This promotes a “smoothing” effect through repeated deformation, rather than “knocking out” new traces.

New “dimples” are made on the shot peened surface, which increase the surface roughness parameter Sv. (Figure 5). After shot peening of C45 steel samples, the Sv parameter is 170% to 256% higher than before the pre-treatment (Figure 5a).

For surfaces shot peened with HS18-0-1 balls (higher specific weight of balls), there is a greater increase in the Sv parameter than after shot peening with 100Cr6 balls. For both ball materials, increasing the shot peening time to  $t=15$  min results in a decrease in the Sv parameter value for C45 steel samples. Figure 5b shows the effect of vibratory shot peening conditions on the Sv parameter for samples made of 100Cr6 steel. In the case of 100Cr6 steel balls, with increasing shot peening time, deeper traces are made. The material is subjected to cyclic loading for  $t=15$  min, which causes deterioration of the surface quality. When shot peening with HS18-0-1 shot, an increase in shot peening time to  $t=15$  min results in a decrease in the depth of valleys. The balls repeatedly deform the same area, causing the valleys from previous impacts to be “levelled out”, although these changes are very minor. An interesting result is the achievement of different valleys depths depending on the material being machined (C45 steel and 100Cr6 steel), despite a similar initial value of  $Sv \approx 2.0$  μm. For samples made of 100Cr6 steel, an increase was obtained

**Table 4.** Surface topography of 100Cr6 steel after VSP

Time VSP t	Ball material: 100Cr6	Ball material: HS18-0-1
1	 <p>Sa = 0.189 μm; Sz = 4.93 μm Sv = 1.68 μm; Sp = 3.24 μm;</p>	 <p>Sa = 0.174 μm; Sz = 6.74 μm; Sv = 4.05 μm; Sp = 2.68 μm;</p>
15	 <p>Sa = 0.257 μm; Sz = 4.12 μm Sv = 2.16 μm; Sp = 1.96 μm;</p>	 <p>Sa = 0.245 μm; Sz = 6.75 μm Sv = 3.85 μm; Sp = 2.90 μm;</p>

**Table 5.** Summary of 3D surface roughness parameters after vibratory shot peening of C45 and 100Cr6 steel using different processing parameters

Steel	Ball material	Time, min	Sa, μm	Sz, μm	Sv, μm	Sp, μm
C45	100Cr6	1	1.03 ± 0.038	12.50 ± 0.500	7.63 ± 0.280	5.33 ± 0.280
		15	0.94 ± 0.049	10.47 ± 0.427	6.31 ± 0.062	4.43 ± 0.255
	HS18-0-1	1	1.09 ± 0.074	13.00 ± 0.322	8.33 ± 0.334	4.34 ± 0.065
		15	1.03 ± 0.024	11.08 ± 0.772	6.80 ± 0.652	4.17 ± 0.425
100Cr6	100Cr6	1	0.19 ± 0.012	4.71 ± 0.189	1.59 ± 0.159	2.76 ± 0.554
		15	0.24 ± 0.015	4.40 ± 0.354	2.04 ± 0.112	1.97 ± 0.126
	HS18-0-1	1	0.17 ± 0.008	6.63 ± 0.196	3.95 ± 0.096	2.57 ± 0.193
		15	0.26 ± 0.010	6.69 ± 0.137	3.86 ± 0.026	1.53 ± 0.135

only for three sets of conditions (100Cr6 balls and  $t = 15$  min, and HS18-0-1 balls and  $t = 1$  min and  $t = 15$  min), while for samples made of C45 steel, an increase was obtained for all treatment conditions. This means that the hardness of the material being processed affects the shot peening results.

The use of balls with a higher specific weight results in a greater reduction in the height of micro-irregularities after pre-treatment. When using HS18-0-1 balls, regardless of the type of

material being processed, lower Sp values were obtained than after shot peening with 100Cr6 balls (Figure 6). Unfortunately, for the C45 steel samples, new peaks were “knocked out”, which deteriorate the surface quality. The Sp parameter for samples from C45 after vibratory shot peening is 30% to 65% higher than before VSP (Figure 6a). In the case of 100Cr6 steel samples after VSP, the Sp parameter is lower than before shot peening (Figure 6b). As a result of the balls

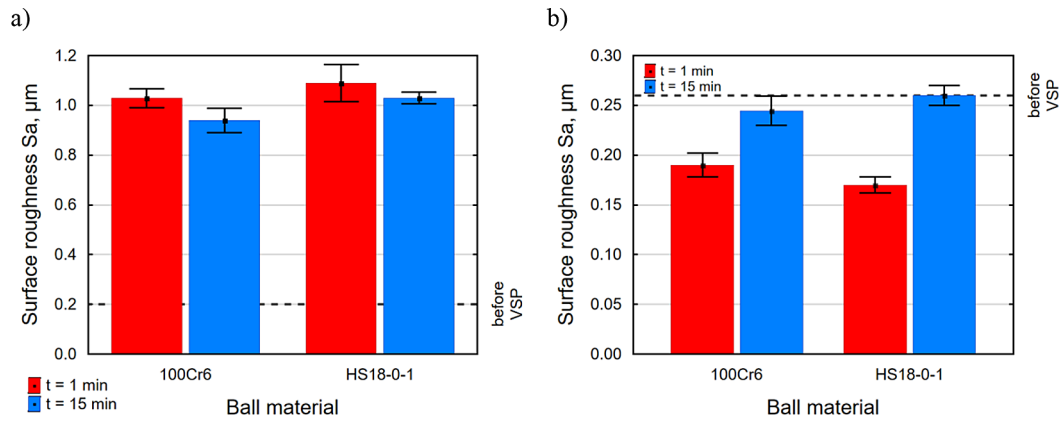


**Figure 3.** Influence of ball material on the surface roughness parameter  $S_a$  for samples a) made of C45 steel, b) made of 100Cr6 steel

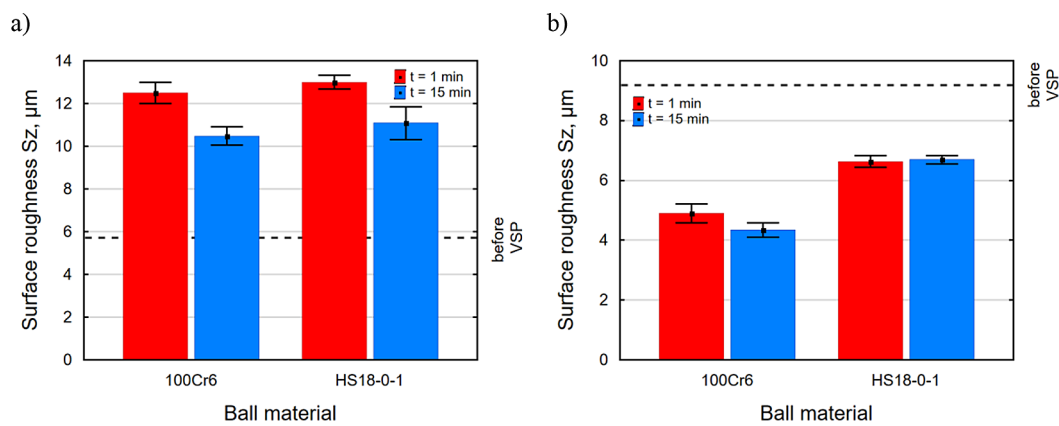


**Figure 4.** Influence of ball material on the surface roughness parameter  $S_z$  for samples a) made of C45 steel, b) made of 100Cr6 steel

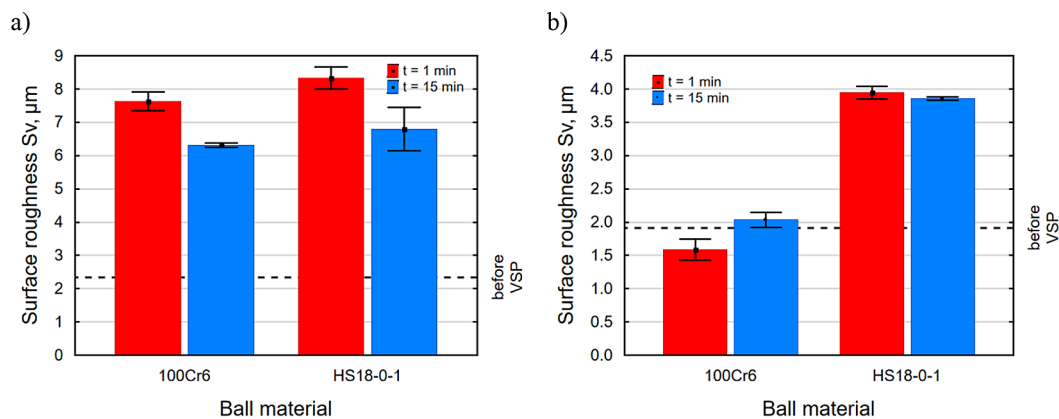


**Figure 5.** Influence of ball material on the surface roughness parameter  $S_v$  for samples a) made of C45 steel, b) made of 100Cr6 steel

hitting the micro-irregularities, they are cut off, flattened and deformed, which reduces the height of the highest peak. After vibratory shot peening of 100Cr6 steel samples, the  $S_p$  parameter is between 2.6 and 3.8 – times lower than before VSP.

Differences in the  $S_p$  parameter value are related to the hardness of the material being processed. After heat treatment, 100Cr6 steel is more than twice as hard as C45, which “hinders” deformation. When analysing the impact of shot peening



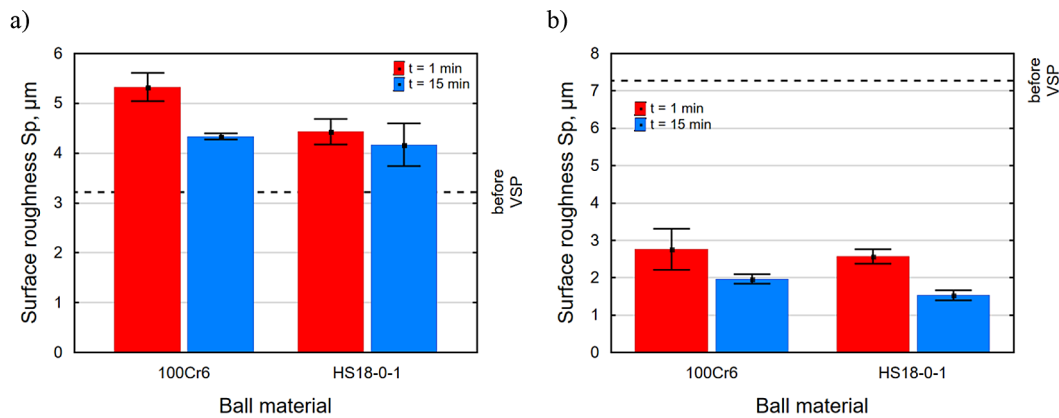


**Figure 6.** Influence of ball material on the surface roughness parameter  $S_p$  for samples a) made of C45 steel, b) made of 100Cr6 steel

time, regardless of the type of material being processed and the material of the balls, an increase in time causes a decrease in the  $S_p$  parameter. In the case of C45 steel samples, a greater influence of time and ball material on the maximum surface micro-irregularities height was observed than in the case of 100Cr6 steel samples.

The surface quality analysis showed that the type of shot peening medium, shot peening time and the material being processed affect the surface roughness parameters. It should be noted that for samples made of 100Cr6 steel, lower surface roughness parameters were obtained after vibratory shot peening than for samples made of C45. The results obtained are similar to those presented in [22, 23], where both an increase and a decrease in roughness parameters were obtained after vibratory shot peening. The use of balls with a higher specific weight (balls made of HS 18-0-1) results in an increase in the surface roughness parameters  $S_a$ ,  $S_z$  and  $S_v$ , with the exception of the  $S_p$  parameter. An increase in the shot peening time to  $t=15 \text{ min}$  translates into a reduction in the maximum height of micro-irregularities, as well as the depth of the valley and the height of the peak.

### Microhardness

The impact of the balls on the surface during vibratory shot peening results in changes in microhardness. During shot peening, the energy of the impact is transferred to the workpiece, which is converted into plastic deformation energy. This promotes an increase in dislocation density, resulting in changes in microhardness. Figure 7 and Table 6 shows the microhardness on the surface of the samples as a function of the vibratory

shot peening conditions applied. For C45 steel samples, a greater increase in microhardness was obtained than for 100Cr6 steel samples. The microhardness increase for C45 is  $\Delta\text{HV}_{0.5}=34\div60$ , while for 100Cr6 it is  $\Delta\text{HV}_{0.5}=6\div18$ . A greater increase in microhardness was obtained for surfaces shot peened with HS18-0-1 balls. This can be explained by the greater specific weight of the balls, which translates into greater impact energy, causing greater deformation. When analyzing the effect of shot peening time on microhardness changes, for  $t=15 \text{ min}$ , the degree of hardening  $e$  ranges from 6.5% to 27.5%, while for  $t=1 \text{ min}$ ,  $e = 2.7\div21.7\%$ . It should be noted that for 100Cr6 steel after heat treatment, microhardness changes are smaller than for C45, which is related to the hardness of the material. The highest increase in microhardness was obtained for the C45 steel sample shot peened at  $t=15 \text{ min}$  using HS18-0-1 shot, which is higher than in previous work [38], but at a similar level to that obtained after centrifugal shot peening [18].

### Residual stress

In the surface layer of the tested samples, prior to the vibratory shot peening process, there are residual stresses of varying signs. For C45 steel samples, these are compressive residual stresses ( $\sigma=-142\pm17 \text{ MPa}$ ), while for samples made of 100Cr6 steel after heat treatment, they are tensile residual stresses ( $\sigma=163\pm18 \text{ MPa}$ ), which are most likely the result of uneven cooling and phase transformations during the hardening process. After vibratory shot peening of C45 steel samples, the absolute value of residual stresses increases (they are still compressive), while in the case of 100Cr6 steel,

**Table 6.** Microhardness after vibratory shot peening of C45 and 100Cr6 steel using different shot peening parameters

Steel	Ball material	Time, min	HV0.5
C45	100Cr6	1	225.7 ± 13.5
		15	273.9 ± 19.4
	HS18-0-1	1	270.1 ± 9.5
		15	282.9 ± 11.2
	Before vibratory shot peening		221.9 ± 7.8
100Cr6	100Cr6	1	571.2 ± 6.6
		15	579.4 ± 22.5
	HS18-0-1	1	572.0 ± 18.9
		15	583.0 ± 6.8
	Before vibratory shot peening		565.0 ± 17.4

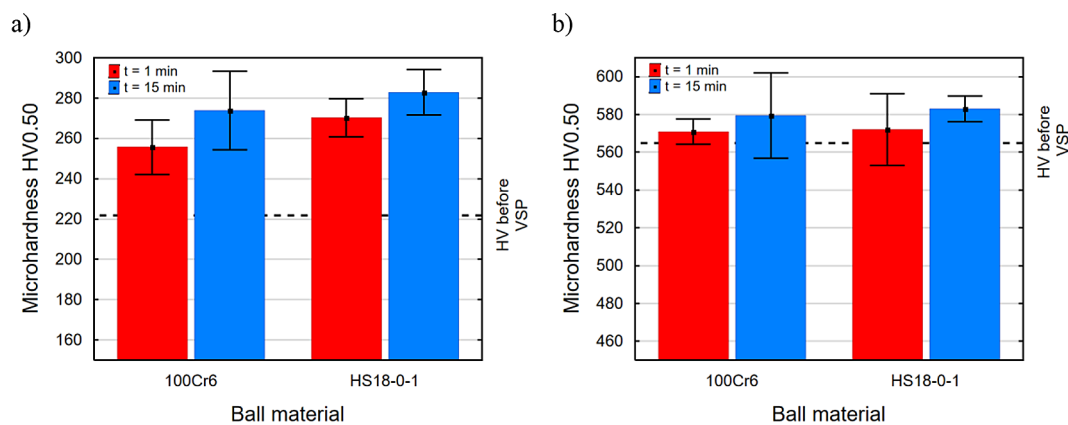


**Figure 7.** Influence of the ball material on the surface microhardness for samples a) made of C45 steel, b) made of 100Cr6 steel

the stress state changes from tensile to compressive. Figure 8 shows and Table 7 the value of residual stresses as a function of shot peening conditions. For both C45 and 100Cr6 steel, shot peening with HS18-0-1 balls resulted in residual stresses with a higher absolute value than for 100Cr6 balls, which is related to microhardness. An increase in shot peening time from  $t=1$  min to  $t=15$  min causes an increase in the absolute value of residual stresses. For C45 steel samples, the increase in residual stress is  $\Delta\sigma=111\div221$  MPa, while for 100Cr6 it is  $\Delta\sigma=234\div247$  MPa. For C45 steel samples, during shot peening at  $t=1$  min, there is a noticeable difference between the values of residual stresses after shot peening with 100Cr6 and HS18-0-1 shot. This is caused by intensive treatment with balls of higher specific weight. In the case of  $t=15$  min, a state of “saturation” is most likely to occur, with repeated deformation of the same areas. For samples made of 100Cr6 steel, no such large differences in residual stress values were obtained,

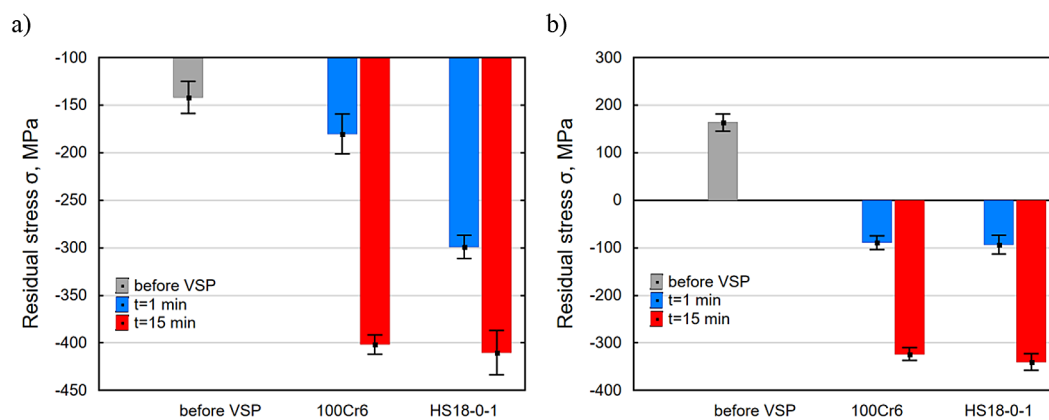
which should be related to the hardness of the shot-peened material. The obtained values of residual stresses for C45 steel samples are slightly lower than those obtained after centrifugal shot peening of the same material [18].

## ANOVA ANALYSIS

A two-factor ANOVA was performed to demonstrate statistically significant differences in surface quality depending on the vibratory shot peening conditions. The dependent variable was the surface roughness parameter  $R_a$ , while the qualitative factors were the shot peening time (A) and the balls material (B). An analysis was also carried out to confirm the existence of interactions between qualitative factors. Table 4 presents the results of the analysis. For both C45 and 100Cr6 steel items, the processing conditions have a significant impact on surface roughness.

**Table 7.** Residual stresses after vibratory shot peening of C45 and 100Cr6 steel using different shot peening parameters

Steel	Ball material	Time, min	$\sigma$ , MPa
C45	100Cr6	1	$-181 \pm 21.0$
		15	$-402 \pm 10.2$
	HS18-0-1	1	$-299 \pm 12.2$
		15	$-410 \pm 23.4$
	Before vibratory shot peening		$-142 \pm 16.9$
100Cr6	100Cr6	1	$-89 \pm 14.4$
		15	$-324 \pm 13.1$
	HS18-0-1	1	$-93 \pm 19.6$
		15	$-340 \pm 17.7$
	Before vibratory shot peening		$163 \pm 18.4$

**Figure 8.** Influence of ball material on residual stresses  $\sigma$  for samples a) made of C45 steel, b) made of 100Cr6 steel

The probability level  $p$  is lower than the significance level  $\alpha=0.05$ . When analysing the partial eta-squared index, it should be noted that the shot peening time, both for C45 and 100Cr6 steel samples, has less influence on the  $R_a$  surface roughness parameter than the type of ball material. There

is an interaction between the vibratory shot peening conditions used for both C45 and 100Cr6 steel samples, as confirmed by the data in Table 8 and Figure 9. The greater “combined” effect of shot peening time (A) and ball material (B) occurs for samples made of 100Cr6 steel than for C45 steel.

**Table 8.** Results of a two-factor ANOVA analysis of the effect of shot peening time (A) and ball material (B) on the surface roughness parameter  $R_a$ 

Material – C45 steel						
Variable	SS	df	MS	F	p	Partial eta-squared
Shot peening time (A)	0.0525	1	0.0525	66.89	0.0000	0.65010
Ball material (B)	0.1729	1	0.1729	220.05	0.0000	0.85940
A*B	0.0297	1	0.0297	37.80	0.0000	0.51217
Material –100Cr6 steel						
Variable	SS	df	MS	F	p	Partial eta-squared
Shot peening time (A)	0.0027	1	0.0027	21.23	0.0000	0.37095
Ball material (B)	0.0005	1	0.0005	43.14	0.0000	0.54511
A*B	0.0075	1	0.0075	59.54	0.0000	0.62321



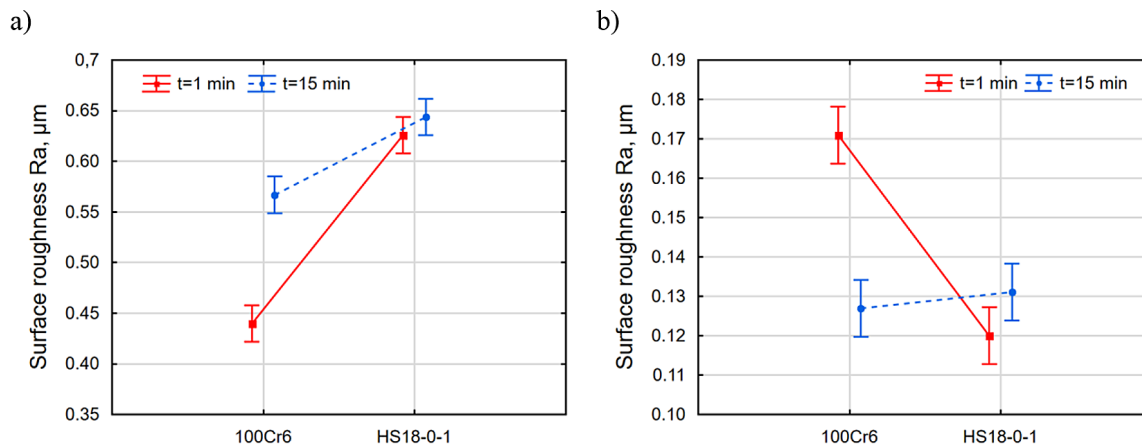


**Figure 9.** Graph of average Ra surface roughness values for the interaction effect between vibratory shot peening time (A) and ball material (B) for samples made of steel a) C45, b) 100Cr6

## CONCLUSIONS

The study investigated the effect of ball material and vibratory shot peening time on the properties of the surface layer of C45 steel and 100Cr6 steel after heat treatment. The following conclusions summarise the results of the study:

- the type of vibratory shot peening material affects the topography, surface roughness parameters, microhardness and residual stresses,
- after vibratory shot peening, the 3D surface roughness parameters for C45 steel samples are higher, while for 100Cr6 steel they are lower than before VSP,
- ANOVA analysis showed that surface roughness significantly depends on the ball material and shot peening time; there is also an interaction between the qualitative factors. The analysis showed that the ball material has a greater impact on the Ra surface roughness parameter than the shot peening time,
- the use of vibratory shot peening causes an increase in microhardness, which for C45 steel samples is  $\Delta\text{HV}_{0.5}=34\div60$ , while for 100Cr6 it is  $\Delta\text{HV}_{0.5}=6\div18$ ; after shot peening with HS18-0-1 balls, the changes in microhardness are greater than after shot peening with 100Cr6 balls,
- compressive residual stresses occur in the surface layer of vibratory shot-peened C45 and 100Cr6 steel objects, and their values are as follows: for C45:  $\sigma = -181$  to  $-410$  MPa, and for 100Cr6  $\sigma = -89 \div -340$  MPa. Higher absolute values of compressive residual stresses were obtained after VSP with HS18-0-1 balls.

In terms of surface quality (low surface roughness), the vibratory shot peening process for both C45 steel components and heat-treated 100Cr6 steel should be carried out using balls made of 100Cr6. However, considering the microhardness on the surface and residual stresses, it is recommended that the VSP process be conducted with balls made of HS18-0-1.

## REFERENCES

- Liu Y.-X., Chen H., Wang R.-Z., Jia Y.-F., Zhang X.-C., Cui Y., Tu S.-T. Fatigue behaviors of 2205 duplex stainless steel with gradient nanostructured surface layer. *International Journal of Fatigue*, 2021; 147: 106170. <https://doi.org/10.1016/j.ijfatigue.2021.106170>
- Novovic D., Dewes R.C., Aspinwall D.K., Voice W., Bowen P. The effect of machined topography and integrity on fatigue life. *International Journal of Machine Tools & Manufacture*, 2004; 44: 125–134. <https://doi.org/10.1016/j.ijmachtools.2003.10.018>
- Kaldunski P., Patyk R., Kukiela L., Bohdal L., Chodor J., Kulakowska A. Numerical analysis and experimental researches of the influence of technological parameters burnishing rolling process on fatigue wear of shafts. *AIP Conf. Proc.* 2019; 2078: 020082, <https://doi.org/10.1063/1.5092085>
- Avcu Y.Y., Iakovakis E., Guney M., Çalın E., Özkılınç A., Abakay E., Sönmez F., Koç F.G., Yamanoglu R., Cengiz A., et al. Surface and tribological properties of powder metallurgical Cp-Titanium alloy modified by shot peening. *Coatings*, 2023; 13, 89. <https://doi.org/10.3390/coatings13010089>
- Vrublevskyi O., Olejniczak K., Napiorkowski J.,

- Gonera J. Modeling wear of different surface layers of agricultural tools in soil abrasive mass. *Measurement*, 2025; 242, Part C: 116076. <https://doi.org/10.1016/j.measurement.2024.116076>
6. Yazdani F., Rabiee S.M., Jamaati R. Comparison of conventional and severe shot peening effects on the microstructure, texture, roughness, hardness, and electrochemical behavior of austenitic stainless steel. *Heliyon*, 2024; 10: e31284. <https://doi.org/10.1016/j.heliyon.2024.e31284>
7. Ciecinska B., Homik W., Matuszak Z. The selection of the parameters of laser beam for constitution of the corrosion resistant surfaces in parts of the rubber vibration damper. *Solid State Phenomena*, 2015; 236: 93 – 97. <https://doi.org/10.4028/www.scientific.net/SSP.236.93>
8. Peng Q., Ming T., Yaolei Han Y., Zhang T. Role of residual stress and ultrafine grain layer at the surface introduced by water jet cavitation peening in stress corrosion cracking of alloy 600 in high temperature water. *Surface and Coatings Technology*, 2025; 496: 131675, <https://doi.org/10.1016/j.surfcoat.2024.131675>.
9. Rudawska A., Miturska I., Szabelski J., Skoczylas A., Drożdżel P., Bociąga E., Madleńak R., Kasperek D. Experimental research and statistic analysis of polymer composite adhesive joints strength. *Journal of Physics: Conference Series* 2017; 842(1): 012074. <https://doi.org/10.1088/1742-6596/842/1/012074>
10. Skoczylas A., Kłonica, M. Selected properties of the surface layer of C45 steel samples after slide burnishing. *Materials*, 2023; 16: 6513. <https://doi.org/10.3390/ma16196513>
11. Ciecinska B., Mucha J. Experimental analysis of the impact of selected laser processing parameters on wettability and surface free energy of EN AW-2024 and EN AW-5083 aluminum alloys. *Advances in Science and Technology Research Journal*, 2025; 19(2): 179–191.
12. <https://doi.org/10.12913/22998624/196012>
13. Lesyk D.A., Martinez S., Morduk B.N., Dzhemelinskiy V.V., Lamikiz A., Prokopenko G.I., Iefimov M.O., Grinkevych K.E. Combining laser transformation hardening and ultrasonic impact strain hardening for enhanced wear resistance of AISI 1045 steel. *Wear*, 2020; 462–463: 203494. <https://doi.org/10.1016/j.wear.2020.203494>
14. Sun W., Wu N., Shao X., Deng L., Li Y., Wang B., Zhang J. The effects of different strengthening treatments on wear performance of ZL109 aluminum alloy at high temperature. *Wear*, 2024; 558–559: 205592. <https://doi.org/10.1016/j.wear.2024.205592>
15. Labuda W., Wieczorska A. Possibility of using the hydrostatic burnishing process under marine conditions. *Advances in Science and Technology Research Journal*, 2024; 18(6): 189–205. <https://doi.org/10.12913/22998624/191543>
16. Patyk R., Kukiela L., Kukiela K., Kułakowska A., Malag L., Bohdal Ł. Numerical study of the influence of surface regular asperities prepared in previous treatment by embossing process on the object surface layer state after burnishing. *Applied Mechanics and Materials*, 2014; 474: 448–453. <https://doi.org/10.4028/www.scientific.net/AMM.474.448>
17. Jambor M., Trško L., Šulak I., Šiška F., Bagherifard S., Guagliano M., Florkova Z. Application of shot peening to improve fatigue properties via enhancement of precipitation response in high-strength Al–Cu–Li alloys. *Journal of Materials Research and Technology*, 2024; 33: 9595–9602. <https://doi.org/10.1016/j.jmrt.2024.11.260>
18. Okuniewski W., Walczak M., Szala M. Effects of shot peening and electropolishing treatment on the properties of additively and conventionally manufactured Ti6Al4V alloy: A review. *Materials*, 2024; 17: 934. <https://doi.org/10.3390/ma17040934>
19. Skoczylas A., Zaleski K. Study on the surface layer properties and fatigue life of a workpiece machined by centrifugal shot peening and burnishing. *Materials*, 2022; 15: 6677. <https://doi.org/10.3390/ma15196677>
20. Zhang X., Wei D., Liu X., Xiao J., Yang S. Effect of compressive residual stress and surface morphology introduced by shot peening on the improvement of fretting fatigue life of TC4. *International Journal of Fatigue*, 2025; 194: 108835. <https://doi.org/10.1016/j.ijfatigue.2025.108835>
21. Zhao J., Tang J., Liu H., Zhang H., Li X., Ding H. High-precision simulation and experimental verification of residual stress and surface topography of cylindrical surface shot peening. *Chinese Journal of Aeronautics*, 2024; 37(9): 535–559. <https://doi.org/10.1016/j.cja.2024.01.019>
22. Niu Z., Men H., Wang C., Gai P., Zhou W., Chen G., Fang Z., Fu X. Effect of surface high density twin microstructure induced by shot peening on the fatigue behavior of Ti-6Al-4V. *Journal of Materials Research and Technology*, 2024; 30: 1806–1821. <https://doi.org/10.1016/j.jmrt.2024.03.234>
23. Patila T., Karunakaran R., Bobaruc F., Sealy M.P. Shot peening induced corrosion resistance of magnesium alloy WE43. *Manufacturing Letters*, 2022; 33: 190–194. <https://doi.org/10.1016/j.mfglet.2022.07.025>
24. <https://doi.org/10.1016/j.mfglet.2022.07.025>
25. Dong F., Peng X., Lai T., Guan C., Li G., Liu J., Dai Y. Improving the surface quality and its mechanism in ultraprecision machining of Al–Mg–Si alloy by multiple high energy shot peening pretreatment. *Journal of Materials Research and Technology* 2024; 30: 7051–7064. <https://doi.org/10.1016/j.jmrt.2024.05.078>

26. Matuszak J., Ciecieląg K., Skoczylas A., Zaleski K. The influence of shot peening and brushing on the deburring effectiveness and surface layer properties of 1.0503 steel. [in:] *Lecture Notes in Mechanical Engineering. Advances in Manufacturing IV. Vol. 1- Mechanical Engineering: Digitalization, Sustainability and Industry Applications*. Springer Nature Switzerland AG 2024; 165–175. <https://doi.org/10.1007/978-3-031-56463-5>
27. Kulisz M., Zagórski I., Matuszak J., Kłonica, M. Properties of the surface layer after trochoidal milling and brushing: Experimental and artificial neural network simulation. *Applied Sciences* 2020; 10(1): 1–26. <https://doi.org/10.3390/app10010075>
28. Ciecieląg K. Use of brushing for improving the surface quality of fiber-reinforced plastics after milling. [in:] *9<sup>th</sup> International Workshop on Metrology for AeroSpace (MetroAeroSpace) - IEEE 2022: proceedings*. 2022: 87–91. <https://doi.org/10.1109/MetroAeroSpace54187.2022.9856281>
29. Matuszak J., Zaleski K., Ciecieląg K., Skoczylas A. Analysis of the effectiveness of removing surface defects by brushing. *Materials* 2022; 15: 7833. <https://doi.org/10.3390/ma15217833>
30. Xiao H., Liu X., Lu Q., Hu T., Yue Hong Y., Li C., Zhong R., Chen W. Promoted low-temperature plasma nitriding for improving wear performance of arc-deposited ceramic coatings on Ti6Al4V alloy via shot peening pretreatment. *Journal of Materials Research and Technology* 2022; 19: 2981–2990. <https://doi.org/10.1016/j.jmrt.2022.06.067>
31. Hotz H., Kirsch B., Zhu T., Smaga M., Beck T., Aurich J.C.: Surface layer hardening of metastable austenitic steel. Comparison of shot peening and cryogenic turning. *Journal of Materials Research and Technology* 2020; 9(6):16410–16422. <https://doi.org/10.1016/j.jmrt.2020.11.109>
32. Okuniewski W., Walczak M., Chocyk D. Properties of the surface layer of titanium alloy Ti-6Al-4V produced by direct metal laser sintering technology after the shot peening treatment. *Advances in Science and Technology Research Journal*, 2025; 19(1): 25–35.
33. <https://doi.org/10.12913/22998624/194860>
34. Zhang P., Lindemann J. Influence of shot peening on high cycle fatigue properties of the high-strength wrought magnesium alloy AZ80. *Scripta Materialia* 2005; 52: 485–490.
35. <https://doi.org/10.1016/j.scriptamat.2004.11.003>
36. Zaleski K. The effect of shot peening on the fatigue life of parts made of titanium alloy Ti-6Al-4V. *Eksploatacja i Niezawodność – Maintenance and Reliability* 2009; 4(44): 65–71.
37. Das T., Erdogan A., Kursuncu B., Maleki E., Unal O. Effect of severe vibratory peening on microstructural and tribological properties of hot rolled AISI 1020 mild steel. *Surf. Coat. Technol.* 2020; 403: 126383. <https://dx.doi.org/10.1016/j.surfcoat.2020.126383>
38. Zaleski K.: The effect of vibratory and rotational shot peening and wear on fatigue life of steel. *Eksploatacja i Niezawodność - Maintenance and Reliability* 2017; 19/1: 102–107. <https://doi.org/10.17531/ein.2017.1.14>
39. Wang S., Chen J., Liu Z., Morgan M., Liu X. Novel contact force measurement in vibratory finishing. *Powder Technology* 2023; 415: 118158. <https://doi.org/10.1016/j.powtec.2022.118158>
40. Courbon C., Valiorgue F., Claudin C., Jacquier M., Dumont F., Rech J. Influence of some superfinishing processes on surface integrity in automotive industry. *Procedia CIRP* 2016; 45: 99–102. <https://doi.org/10.1016/j.procir.2016.02.345>
41. Gopinath A., Teoh J.W., Tagade P., Khoon G.L.E., Haubold T., Kumar A.S. Smart vibratory peening: An approach towards digitalization and integration of vibratory special process into smart factories. *Engineering Applications of Artificial Intelligence*, 2023; 126, Part D: 107118. <https://doi.org/10.1016/j.engappai.2023.107118> Get rights and content
42. Skoczylas A., Zaleski, K. The effect of the chamber-filling ratio in vibratory shot peening on selected surface layer properties of 30HGSA. *Materials* 2025; 18: 8. <https://doi.org/10.3390/ma18010008>
43. Matuszak J. Analysis of geometric surface structure and surface layer microhardness of Ti6Al4V titanium alloy after vibratory shot peening. *Materials* 2023; 16: 6983. <https://doi.org/10.3390/ma16216983>
44. Kumar D., Idapalapati S., Wang W., Child D.J., Haubold T., Wong C.C. Microstructure-mechanical property correlation in shot peened and vibro-peened Ni-based superalloy. *Journal of Materials Processing Technology*, 2019; 267: 215–229. <https://doi.org/10.1016/j.jmatprotec.2018.12.007>
45. Skoczylas A. The effect of vibratory shot peening on the geometric structure of the surface of elements machined by laser and abrasive water jet cutting. *Advances in Science and Technology Research Journal* 2023; 17(5): 1–11. <https://doi.org/10.12913/22998624/170970>